Available online at www.sciencedirect.com
ScienceDirect
International Journal of Thermal Sciences 46 (2007) 20–29
International Journal of Thermal Sciences
www.elsevier.com/locate/ijts

Numerical analysis of convection conduction and radiation using a non-equilibrium model in a square porous cavity

Irfan Anjum Badruddin [a,*], Z.A. Zainal [a], P.A. Aswatha Narayana [b], K.N. Seetharamu [b]

[a] *School of Mechanical Engineering, Universiti Sains Malaysia 14300 Nibong Tebal, Pulau Pinang, Malaysia*
[b] *MS Ramaiah School of Advanced Studies, Gnanagangothri Campus, New BEL Road, Bangalore 560 054, India*

Received 4 October 2005; received in revised form 8 March 2006; accepted 9 March 2006

Available online 8 June 2006

Abstract

Numerical analysis of heat transfer by convection, conduction and radiation in a saturated porous medium enclosed in a square cavity is investigated using a thermal non-equilibrium model. The flow is assumed to follow Darcy law. The governing partial differential equations are non-dimensionalised and solved numerically using finite element method. The left vertical surface of the square cavity is maintained at an isothermal temperature T_h and the right vertical surface at T_c such that $T_c < T_h$. The top and bottom surfaces of the cavity are assumed to be adiabatic. Results are presented in terms of Nusselt number for fluid, Nusselt number for solid and total Nusselt number, for various parameters such as inter-phase heat transfer coefficient, modified conductivity ratio, radiation parameter and Rayleigh number.

Keywords: Porous media; Square cavity; Free convection; Radiation; Thermal non-equilibrium; FEM

1. Introduction

Heat transfer through porous media has become an intensive research topic for last few decades. The interest in heat transfer through porous media can be attributed to its wide range of applications such as thermal insulation of buildings, heat exchangers, solar energy collectors, geophysical applications, solidification of alloys, nuclear waste disposal drying processes etc, which covers a vast range of engineering and science disciplines. The research literature suggests that a good amount of work has been done to understand the heat transfer behavior in the porous medium. Recent books by Nield and Bejan [1], Vafai [2,3], Pop and Ingham [4] provide a good understanding of the subject and also give the picture of research work carried out in this field. Most of the research dealing with heat transfer in porous media has been dealt by considering that the fluid phase and solid phase of porous media are in thermal equilibrium state. In many applications this assumption of thermal equilibrium does not hold good as the fluid and solid matrix have different temperatures leading to thermally non-equilibrium condition. The study of porous media as a non-equilibrium system has not received as much attention as the equilibrium study has achieved. Baytas and Pop [5] have studied the free convection in a porous cavity using non-equilibrium model by employing the cell-centered finite volume scheme. Saeid [6] has considered the non-equilibrium model to analyse mixed convection in a vertical porous layer by using finite volume method. His study suggests that, for a mixed convection region the total average Nusselt number is more for lower Rayleigh number than that for higher Rayleigh number. Jiang and Ren [7] have investigated the forced convection heat transfer in porous media using a thermal non-equilibrium model. Rees et al. [8] have investigated the forced convection past a heated cylinder in a porous medium by employing thermal non-equilibrium model and found that the heat transfer coefficient do not vary in tangential direction of cylinder when the porous medium is in thermal equilibrium condition but, heat transfer coefficients vary when system comes under thermal non-equilibrium conditions. Wong et al. [9] have supplemented the work of Rees et al. [8] for finite values of Peclet number. An analysis of non-Darcian effects by using two-temperature

* Corresponding author. Tel.: +604 5996369; fax: +604 5941025.
E-mail address: irfan_magami@rediffmail.com (I.A. Badruddin).

1290-0729/$ – see front matter
doi:10.1016/j.ijthermalsci.2006.03.006

Nomenclature

A	area of element	m^2	
c_p	specific heat of fluid	$J\,kg^{-1}\,°C^{-1}$	
g	acceleration due to gravity	$m\,s^{-2}$	
h	convective heat transfer coefficient	$W\,m^{-2}\,°C^{-1}$	
H	inter-phase heat transfer coefficient		
k_s, k_f	solid and fluid thermal conductivity respectively	$W\,m^{-1}\,°C^{-1}$	
K	permeability of porous medium	m^2	
L	height of cavity	m	
n	refractive index		
N_i	shape function		
$Nu, \overline{Nu}$	local Nusselt number and average Nusselt number respectively		
q_r	radiation flux	$W\,m^{-2}$	
R_d	radiation parameter		
Ra	modified Raleigh number		
$T, \overline{T}$	dimensional (°C) and non-dimensional temperature		
u, v	velocity components in x and y direction respectively	$m\,s^{-1}$	
x, y	Cartesian coordinates		
$\bar{x}, \bar{y}$	non-dimensional co-ordinates		

Greek symbols

α	thermal diffusivity	$m^2\,s^{-1}$
β	coefficient of thermal expansion	$1\,°C^{-1}$
γ	modified conductivity ratio	
ρ	density	$kg\,m^{-3}$
ν	coefficient of kinematic viscosity	$m^2\,s^{-1}$
σ	Stephan Boltzmann constant	$W\,m^{-2}K^{-4}$
β_R	Rosseland mean extinction coefficient	$1\,m^{-1}$
φ	porosity	
ψ	stream function	
$\bar{\psi}$	non-dimensional stream function	

Subscripts

h	hot
c	cold
f	fluid
s	solid
t	total

model in a porous media has been carried out by Marafie and Vafai [10]. They found that the temperature difference between fluid and solid phases decreases with increasing Biot number. Cherif and Sifaoui [11,12] and Sghaier et al. [13] have studied the radiation heat transfer in porous media enclosed in a cylindrical and spherical geometry. They have used Runge–Kutta method and finite difference method respectively to solve the governing equations and presented results for fluid as well as solid matrix temperatures. Baytas [14] has considered thermal non-equilibrium model to study the non-Darcy natural convection in a heat generating porous medium.

The present paper concentrates on the study of heat transfer by convection, conduction and radiation in a saturated porous medium confined in a square cavity using a two-temperature thermal non-equilibrium model and thus predicts the temperature of fluid and solid matrix. To the best of our knowledge, the study of heat transfer by convection, conduction and radiation through saturated porous medium confined in a square cavity has not been reported so far. In this study, finite element method has been used to solve the governing partial differential equations. Results are presented in terms of Nusselt number, streamlines and isotherms for various values of the inter-phase heat transfer coefficient, modified conductivity ratio, radiation parameter and Rayleigh number.

2. Analysis

Consider a square cavity filled with saturated porous medium. The schematic of the problem under consideration and coordinate system is shown in Fig. 1. The left vertical surface of the cavity is maintained at temperature T_h which is greater than the right vertical surface temperature T_c. The top and bottom horizontal surfaces of cavity are adiabatic. The following assumptions are applied:

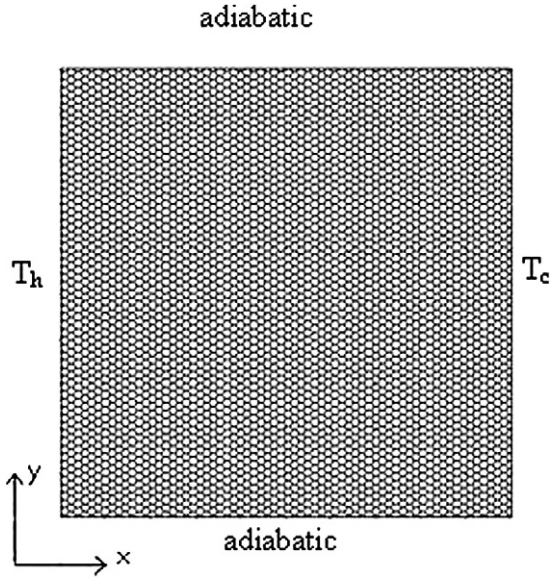

Fig. 1. Schematic diagram of the square cavity.

(a) The flow inside the porous medium is assumed to obey Darcy law.
(b) The convective fluid and the porous medium are not in local thermodynamic equilibrium thus allowing fluid and solid matrix to have different temperatures.
(c) There is no phase change of the fluid in the medium.
(d) The properties of the fluid and those of the porous medium are homogeneous and isotropic.

(e) Fluid properties are constant except the variation of density with temperature.
(f) The fluid is transparent to radiation.
(g) The medium behaves as an optically thick gray body and the radiative heat flux in the y-direction is negligible in comparison to that in the x-direction.

With above assumptions, the governing equations for fluid flow are given as:

Continuity equation

$$\frac{\partial u}{\partial x}+\frac{\partial v}{\partial y}=0 \tag{1}$$

Momentum equation

$$\frac{\partial u}{\partial y}-\frac{\partial v}{\partial x}=-\frac{g\beta K}{\nu}\frac{\partial T_f}{\partial x} \tag{2}$$

Energy equation for fluid

$$(\rho c_p)_f\left(u\frac{\partial T_f}{\partial x}+v\frac{\partial T_f}{\partial y}\right) =\varphi k_f\left(\frac{\partial^2 T_f}{\partial x^2}+\frac{\partial^2 T_f}{\partial y^2}\right)+h(T_s-T_f) \tag{3}$$

Energy equation for solid

$$(1-\varphi)k_s\left(\frac{\partial^2 T_s}{\partial x^2}+\frac{\partial^2 T_s}{\partial y^2}\right)=h(T_s-T_f)+(1-\varphi)\frac{\partial q_r}{\partial x} \tag{4}$$

Where u and v are Darcy's velocities in the x and y directions respectively, the boundary conditions are:

$$\text{at } x=0,\quad u=0,\quad v=0,\qquad T_f=T_s=T_h \tag{5a}$$

$$\text{at } x=L,\quad u=0,\quad v=0,\qquad T_f=T_s=T_c \tag{5b}$$

$$\text{at } y=0,L,\quad u=0,\quad v=0,\qquad \partial T_f/\partial y=\partial T_s/\partial y=0 \tag{5c}$$

Eq. (1) can be satisfied by introducing the stream function ψ as:

$$u=\frac{\partial \psi}{\partial y},\qquad v=-\frac{\partial \psi}{\partial x} \tag{6}$$

Following non-dimensional parameters are used to non-dimensionalise the governing equations:

Non-dimensional width

$$\bar{x}=\frac{x}{L}$$

Non-dimensional height

$$\bar{y}=\frac{y}{L}$$

Non-dimensional stream function

$$\bar{\psi}=\frac{\psi}{\varphi\alpha_f} \tag{7}$$

Non-dimensional temperature

$$\overline{T}=\frac{(T-T_o)}{(T_h-T_c)},\quad \text{where } T_o=\frac{(T_h+T_c)}{2}$$

Radiation parameter

$$R_d=\frac{4\sigma n^2 T_c^3}{\beta_R k_s}$$

Rayleigh number

$$Ra=\frac{g\beta\Delta T K L}{\varphi\nu\alpha_f}$$

Inter-phase heat transfer coefficient

$$H=\frac{hL^2}{\varphi k_f}$$

Modified conductivity ratio

$$\gamma=\frac{\varphi k_f}{(1-\varphi)k_s}$$

Invoking the Rosseland approximation for radiation [15] yields.

$$q_r=-\frac{4n^2\sigma}{3\beta_R}\frac{\partial T^4}{\partial x} \tag{8}$$

The non-linear term T^4 in Eq. (8) can be expanded in Taylor series. Expanding T^4 about T_c and neglecting higher order terms [16] results:

$$T^4\approx 4TT_c^3-3T_c^4 \tag{9}$$

Substituting Eqs. (5)–(9) into Eqs. (2)–(4) yields:

$$\frac{\partial^2\bar{\psi}}{\partial\bar{x}^2}+\frac{\partial^2\bar{\psi}}{\partial\bar{y}^2}=-Ra\frac{\partial\overline{T}_f}{\partial\bar{x}} \tag{10}$$

$$\left[\frac{\partial\bar{\psi}}{\partial\bar{y}}\frac{\partial\overline{T}_f}{\partial\bar{x}}-\frac{\partial\bar{\psi}}{\partial\bar{x}}\frac{\partial\overline{T}_f}{\partial\bar{y}}\right] =\left(\frac{\partial^2\overline{T}_f}{\partial\bar{x}^2}+\frac{\partial^2\overline{T}_f}{\partial\bar{y}^2}\right)+H(\overline{T}_s-\overline{T}_f) \tag{11}$$

$$\frac{\partial^2\overline{T}_s}{\partial\bar{x}^2}+\frac{\partial^2\overline{T}_s}{\partial\bar{y}^2}=H\gamma(\overline{T}_s-\overline{T}_f)-\frac{4R_d}{3}\frac{\partial^2\overline{T}_s}{\partial\bar{x}^2} \tag{12}$$

Corresponding boundary conditions are:

$$\text{at } \bar{x}=0,\quad \bar{\psi}=0,\qquad \overline{T}_f=\overline{T}_s=\frac{1}{2} \tag{13a}$$

$$\text{at } \bar{x}=1,\quad \bar{\psi}=0,\qquad \overline{T}_f=\overline{T}_s=-\frac{1}{2} \tag{13b}$$

$$\text{at } \bar{y}=0,1\quad \bar{\psi}=0,\qquad \partial\overline{T}_f/\partial\bar{y}=\partial\overline{T}_s/\partial\bar{y}=0 \tag{13c}$$

The heat transfer rate at cold and hot surfaces of the cavity can be predicted in terms of Nusselt number, which is given as:

For fluid

$$Nu_f=-\left(\frac{\partial\overline{T}_f}{\partial\bar{x}}\right)_{\bar{x}=0,1}\quad\text{and}\quad \overline{Nu}_f=\int_0^1 Nu_f\,\mathrm{d}\bar{y} \tag{14}$$

For solid

$$Nu_s=-\left(\left(1+\frac{4}{3}R_d\right)\frac{\partial\overline{T}_s}{\partial\bar{x}}\right)_{\bar{x}=0,1}\quad\text{and}$$

$$\overline{Nu}_s=\int_0^1 Nu_s\,\mathrm{d}\bar{y} \tag{15}$$

The average total Nusselt number [6] is given by:

$$\overline{Nu}_t = \frac{-1}{1+\gamma}\int_0^1 \left\{ \gamma \left(\frac{\partial \overline{T}_f}{\partial \bar{x}} \right)_{\bar{x}=0,1} + \left(1+\frac{4R_d}{3}\right)\left(\frac{\partial \overline{T}_s}{\partial \bar{x}} \right)_{\bar{x}=0,1} \right\} \mathrm{d}\bar{y} \tag{16}$$

3. Numerical scheme

Eqs. (10)–(12) are coupled partial differential equations in the non-dimensional form, subjected to boundary conditions (13). In order to predict the heat transfer behavior in the porous medium, Eqs. (10)–(12) are to be solved. These equations are solved by using finite element method. The Galerkin method is applied to convert the partial differential equations into matrix form of equations. A simple triangular element with 3 nodes is used to represent variations of the temperature and stream function inside the element. $\overline{T}_f$, $\overline{T}_s$ and $\bar{\psi}$ vary inside the element and can be expressed as:

$$\overline{T}_f = \overline{T}_{f1}N_1 + \overline{T}_{f2}N_2 + \overline{T}_{f2}N_3 \tag{17a}$$

$$\overline{T}_s = \overline{T}_{s1}N_1 + \overline{T}_{s2}N_2 + \overline{T}_{s2}N_3 \tag{17b}$$

$$\bar{\psi} = \bar{\psi}_1 N_1 + \bar{\psi}_2 N_2 + \bar{\psi}_3 N_3 \tag{17c}$$

where N_1, N_2 and N_3 are the shape functions given as:

$$N_i = \frac{a_i + b_i x + c_i y}{2A}, \quad i = 1, 2, 3 \tag{18}$$

In the above equation a_i, b_i, c_i are matrix coefficients.

Details of FEM formulations can be obtained from [17,18]. First, Eqs. (10)–(12) are converted into matrix form of equations for an element. The coupled matrix equations for the elements are assembled to get the global matrix for the whole domain, which is solved iteratively, to obtain $\overline{T}_f$, $\overline{T}_s$ and $\bar{\psi}$ in the porous medium. In order to get accurate results, error level of solution, for $\overline{T}_f$, $\overline{T}_s$ and $\bar{\psi}$ are set at 10^{-5}, 10^{-5} and 10^{-7} respectively. The iterative process is terminated when the above-mentioned error level, which is the difference between previous iteration and the current iteration for a variable at all nodes, is achieved. Element size in the domain varies since smaller size elements are used near the wall and bigger size elements are placed away from the wall. Large number of elements are located near the wall since large variations in $\overline{T}_f$, $\overline{T}_s$ and $\bar{\psi}$ are expected in these regions of the cavity. A sufficiently dense mesh is chosen to make the solution mesh invariant. The variations in results were found to be insignificant when the number of elements is increased from 2596 to 5000, but the time taken to solve 5000 elements was considerably higher as compared to that of 2596 elements. Thus the mesh with 2596 elements is selected in the present study. The domain is meshed in such a way that the elements are placed symmetrical about central horizontal and vertical lines of the cavity. The computations are carried out on a computer with Pentium 4 processor and 2.4 GHz speed.

Table 1
Total average Nusselt number, $\overline{Nu}_t$ comparison

Author	$Ra = 10$	$Ra = 100$
Walker and Homsy [19]		3.097
Bejan [20]		4.2
Gross et al. [21]		3.141
Manole and Lage [22]		3.118
Beckerman et al. [23]		3.113
Moya et al. [24]	1.065	2.801
Baytas and Pop [25]	1.079	3.16
Misirlioglu et al. [26]	1.119	3.05
Present	1.0733	3.2001

4. Results and discussion

Numerical results are presented in terms of local and average Nusselt number, which is a measure of heat transfer rate from the surface. The Nusselt number for fluid Nu_f, solid Nu_s, and the total Nusselt number Nu_t are calculated at both hot and cold walls of the cavity. In order to verify the accuracy of present method, the numerical results obtained from present method for the case of thermal equilibrium model are compared with the results presented by various authors [19–26]. The comparison is shown in Table 1. Results of Table 1 shows that the present method compares well with the results of authors [19,21–23,25] and thus provide confidence to predict heat transfer characteristics of presently considered problem.

Fig. 2 shows the isotherms (fluid and solid) and streamlines for various values of H at $Ra = 100$, $R_d = 0.5$ and $\gamma = 1$. It is obvious from this figure that the non-equilibrium effect is very strong at low values of heat transfer parameter, H. The isotherms of fluid are not much affected due to change in the value of H whereas the isotherms of solid deviate to larger extent when H is increased from 0.1 to 1000. The isotherms for fluid move slightly away from vertical surface when H is increased, indicating reduction in the heat transfer rate at wall. However the isotherms for solid move closer to the vertical surface when H is increased indicating higher thermal gradient and thus higher heat transfer rate from the wall. It may be noted that the increased inter-phase heat transfer coefficient is associated with increased heat transfer between solid and fluid phases. The increased heat transfer between two phases brings their temperature closure to each other thus the fluid and solid isotherms look similar at higher values of H, which reveals that the solid and fluid phases are in a state of thermal equilibrium. The streamlines show that the flow pattern follows the geometry of cavity when H is increased.

Fig. 3 depicts the isotherms and streamlines for various values of γ at $Ra = 100$, $R_d = 0.5$ and $H = 25$. It is evident from this figure that the isotherms of solid are affected to greater degree as compared to the isotherms of fluid when γ is increased. At large value of γ, the isotherms for both the phases become similar. This happens due to fact that non-equilibrium forces are very weak and thus equilibrium prevails at high values of γ. At low values of γ, the isotherms of solid are almost parallel to the vertical wall of cavity. This can be attributed to the reason that low γ is associated with high thermal conductivity of solid for a given porosity and fluid properties. High thermal conductivity

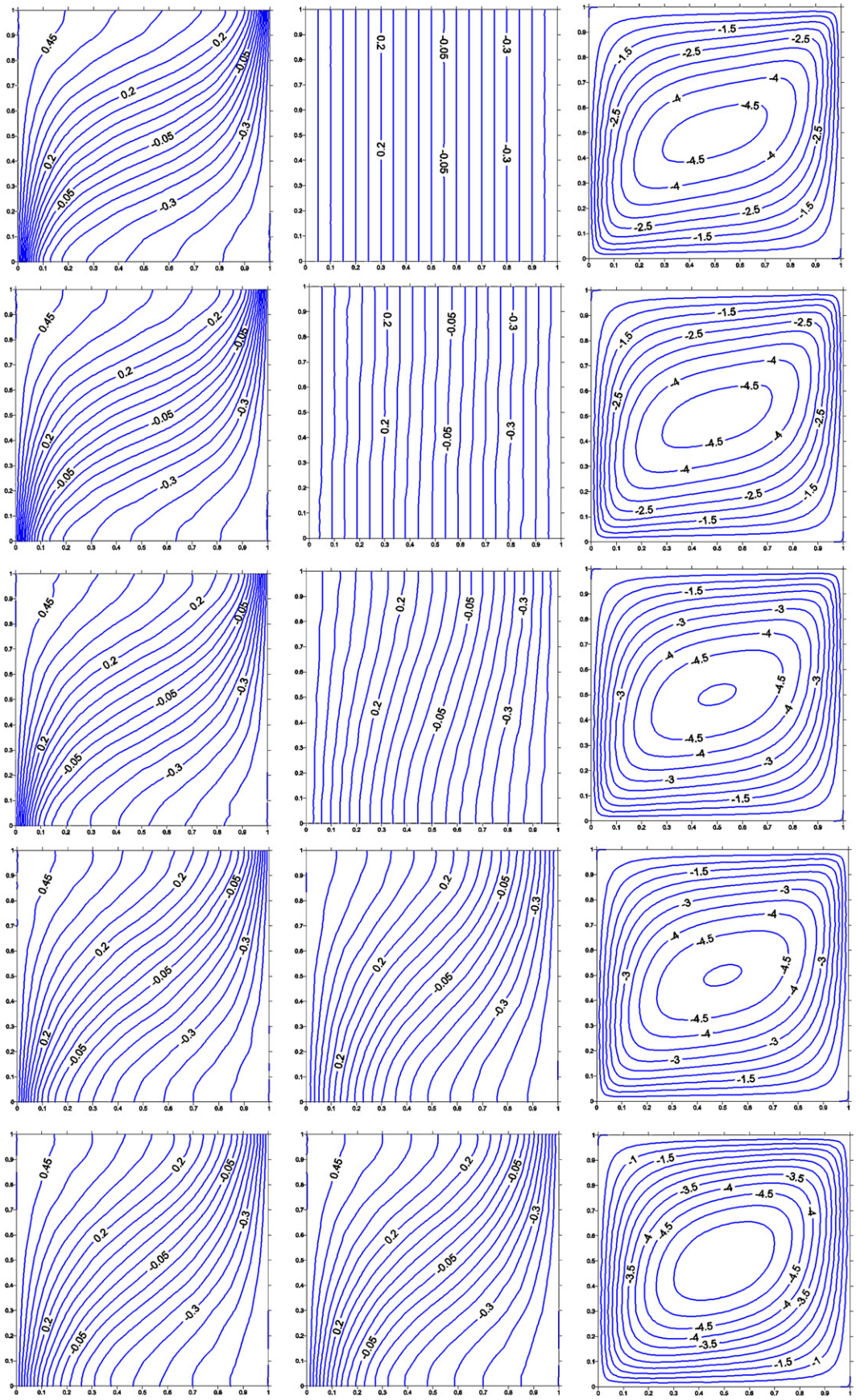

Fig. 2. Isotherms for fluid (left), solid (center) and streamlines (right) at $H = 0.1$, 1, 10, 100 and 1000 (increasing from top towards bottom).

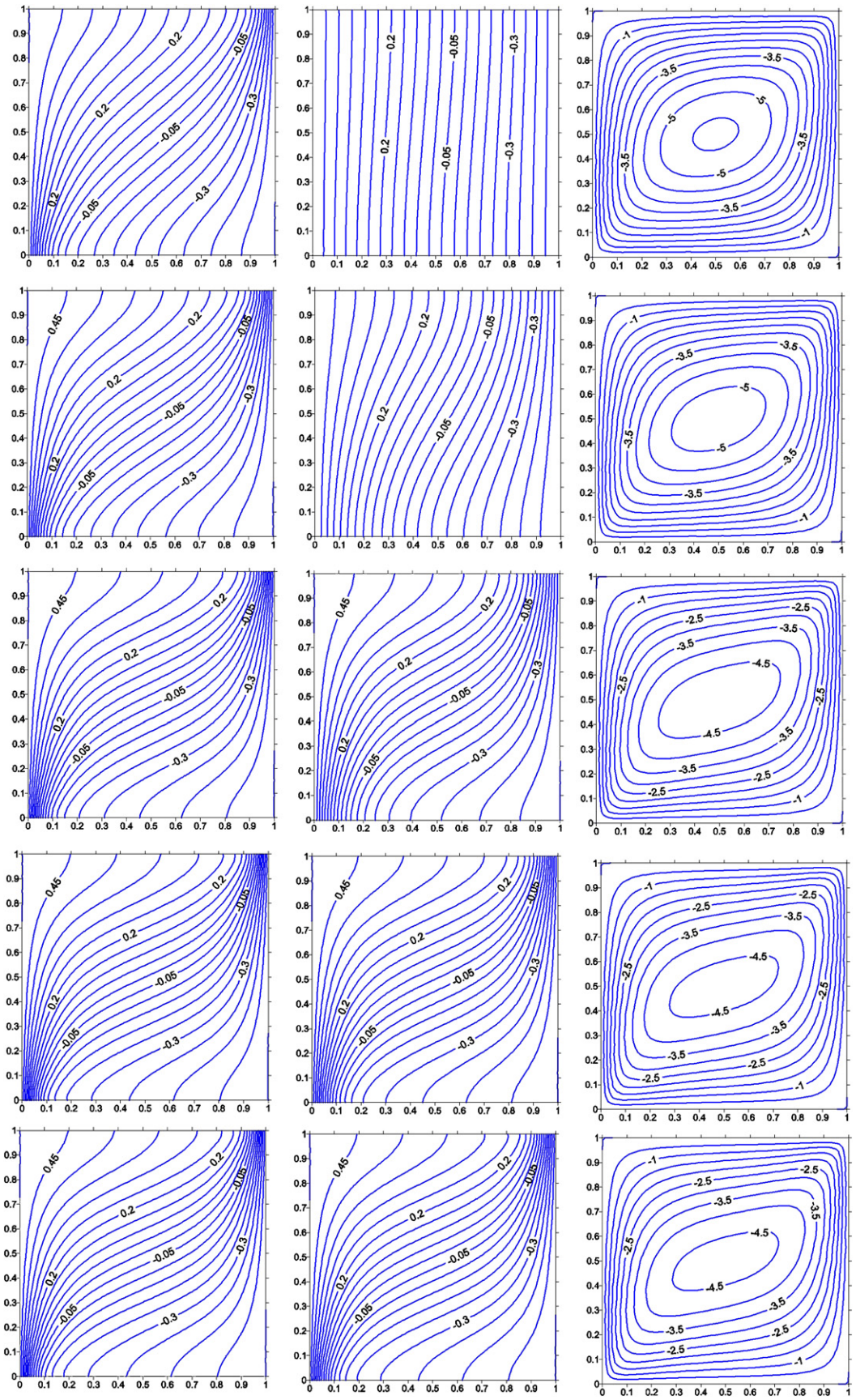

Fig. 3. Isotherms for fluid (left), solid (center) and streamlines (right) at $\gamma = 0.1$, 1, 10, 50 and 100 (increasing from top towards bottom).

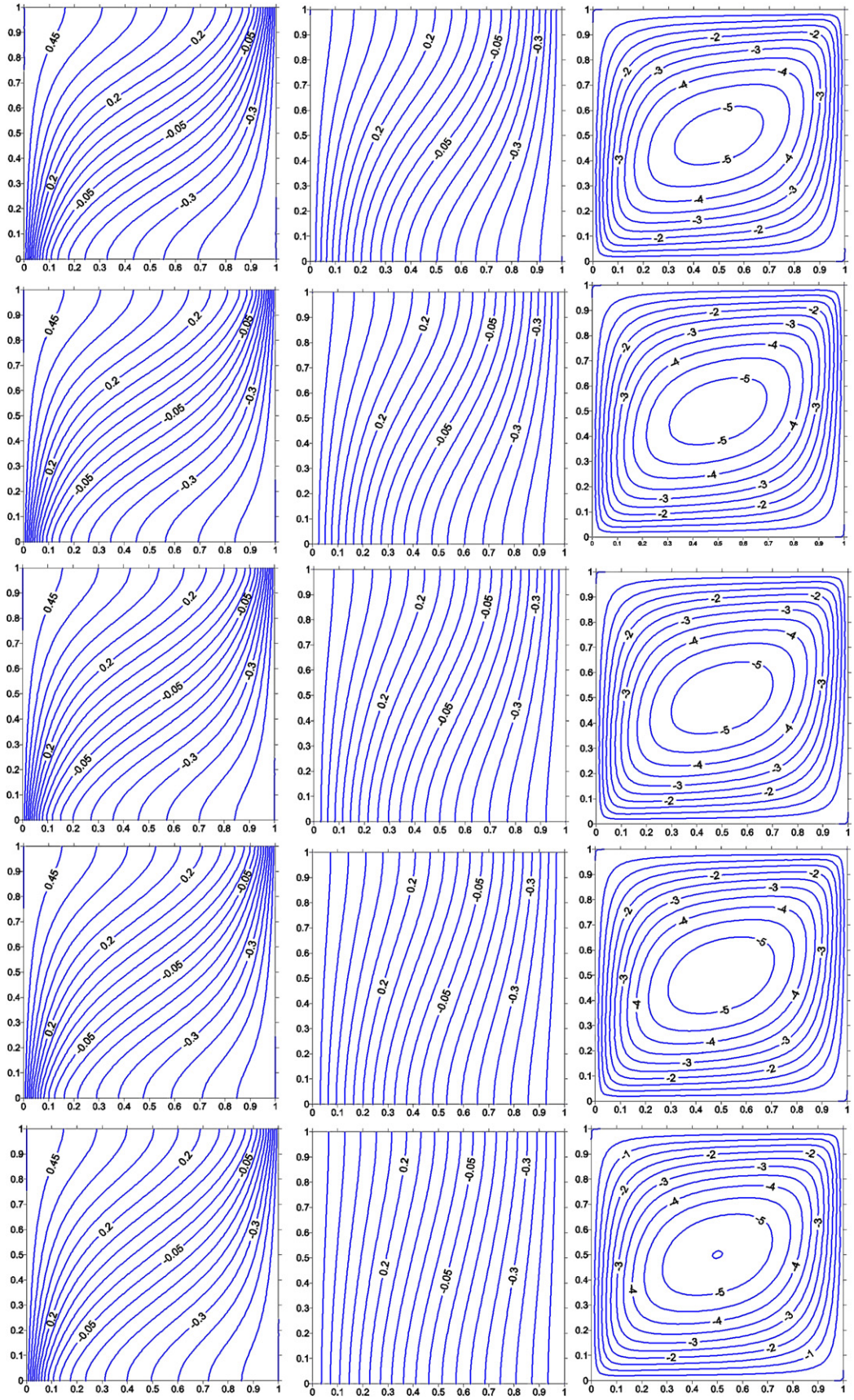

Fig. 4. Isotherms for fluid (left), solid (center) and streamlines (right) at $R_d = 0, 0.5, 1, 2$ and 4 (increasing from top towards bottom).

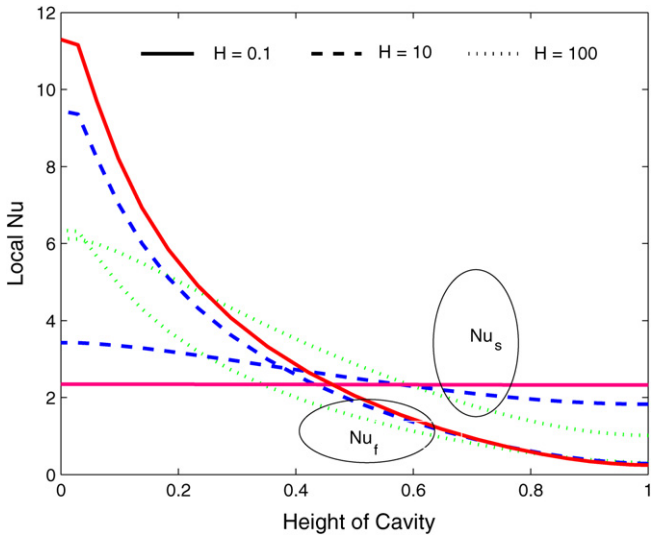

Fig. 5. *Nu* along the height of cavity at hot surface.

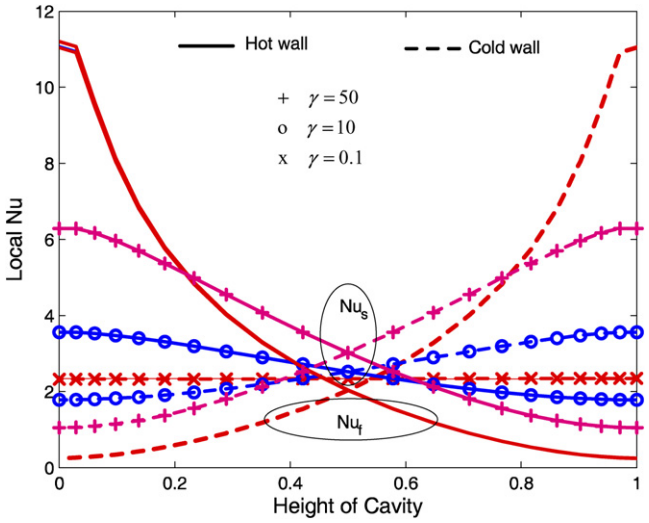

Fig. 6. *Nu* along the height of cavity.

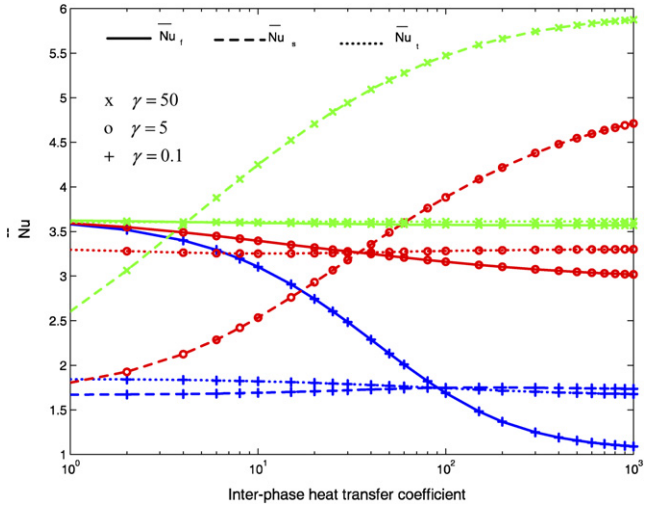

Fig. 7. Average Nusselt number vs H for different values of γ.

of solid leads to low thermal resistance in solid phase and thus heat is distributed evenly throughout the cavity. The isotherms of solid starts crowding near the vertical wall when γ is increased and thus increasing the heat transfer rate from the wall.

Fig. 4 provides information of the isotherms and streamline when radiation parameter is varied. This figure corresponds to the value $Ra = 100$, $H = 25$ and $\gamma = 1$. The isotherms of solid tend to become parallel with the vertical surface of the cavity when radiation parameter is increased. This happens because of the reason that the radiation enhances the conductive heat transfer in the solid. The streamlines follow the geometry of cavity due to smooth upward and downward movement of fluid near the left and right wall of cavity respectively.

Fig. 5 shows the fluid (Nu_f) and solid (Nu_s) local Nusselt numbers at the hot wall of the cavity for $Ra = 100$, $R_d = 1$ and $\gamma = 1$. It can be seen that the local Nusselt number for the fluid and solid phase decreases with an increase of cavity height. Nu_f is higher at the bottom part of cavity as compared to Nu_s and vice versa at upper part of the cavity. Increase in the inter-phase heat transfer coefficient H, leads to decrease in Nu_f at the bottom part of cavity but influence of H diminishes as the height of cavity increases. Increase in H increases the Nu_s at bottom portion of cavity but decrease at upper portion of the cavity. At smaller values of H, the heat transfer between fluid and solid phases is very small thus the heat content of fluid and solid does not affect each other's temperature field. Since the wall is maintained at constant temperature, the heat transferred from wall to solid phase remains constant throughout the height of the cavity which in turn leads to constant Nusselt number of solid throughout the height of the cavity at small (0.1) values of H. It is observed that, due to symmetry the heat transfer rate at cold wall is mirror image as that at the hot wall.

Fig. 6 depicts the Nusselt number for fluid and solid phases at hot and cold walls at various values of modified thermal conductivity ratio γ, for $Ra = 100$, $R_d = 1$ and $H = 1$. There is a negligible effect on Nusselt number of the fluid phase when γ is varied. It can be seen that the curves of Nu_f for $\gamma = 0.1$, 10 and 50, almost overlap each other indicating negligible effect of γ. Thus for $\gamma = 0.1$, 10 and 50, there is only one curve of Nu_f is visible in the figure. Nu_s along the height of cavity decreases at hot wall. However Nu_s increases with the height of cavity at cold wall. At $\gamma = 0.1$, there is not much difference between the values of Nusselt number at hot and cold wall. Thus there is only one curve shown in figure for $\gamma = 0.1$.

Fig. 7 reflects the variations of average Nusselt number with respect to inter-phase heat transfer coefficient H, for different values of γ at $Ra = 100$ and $R_d = 0.5$. It may be noted that the average Nusselt number at hot and cold wall is equal due to symmetry. It is seen that the $\overline{Nu}_f$ decreases with increase in the value of H. The increased inter-phase heat transfer coefficient leads to faster heat transfer from solid phase to fluid phase in the medium, thus increasing the temperature of fluid phase. The increased fluid-phase temperature reduces the temperature difference between fluid and the wall, which in turn retards the heat transfer rate from wall to the fluid phase. Since the Nusselt number describes the surface heat transfer phenomenon thus increased H value reduces the Nusselt number of fluid-phase. The decrease of $\overline{Nu}_f$ is sharp for the value $10 < H < 100$. The vari-

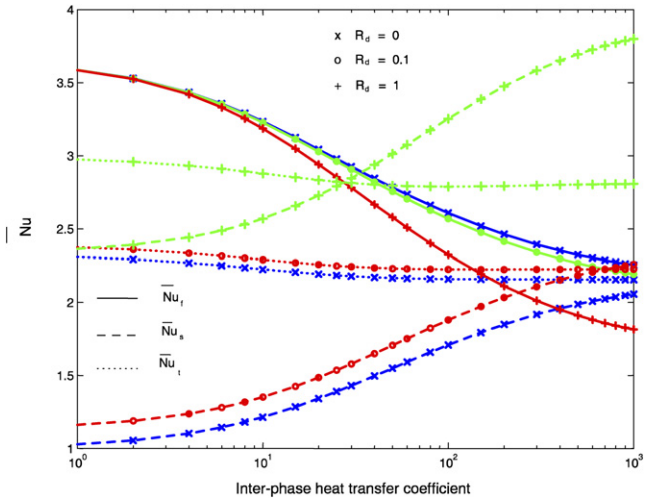

Fig. 8. Average Nusselt number vs H for different values of R_d.

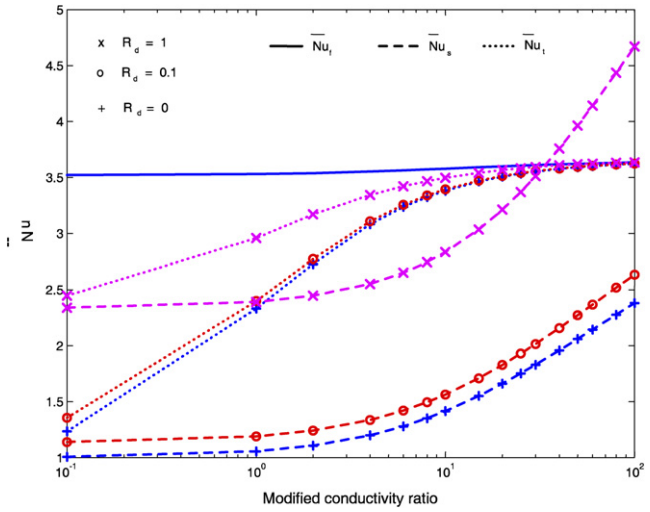

Fig. 9. Average Nusselt number vs γ for different values of R_d.

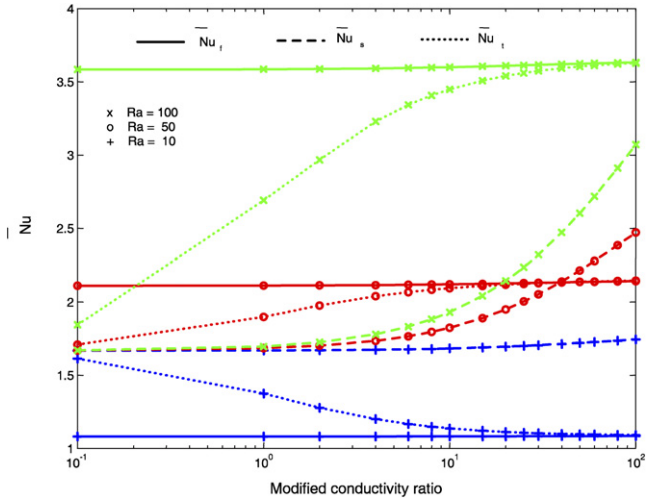

Fig. 10. Average Nusselt number vs γ for different values of Ra.

ation in $\overline{Nu}_f$ with respect to H decreases with increased value of modified thermal conductivity ratio, γ. At $H = 1000$, an increase of 176% in $\overline{Nu}_f$ is observed when γ is varied from 0.1 to 5 whereas $\overline{Nu}_f$ increased by 1.55% when γ is changed from 5 to 50. Nusselt number for solid increases with increase in H. Effect of γ on $\overline{Nu}_s$ is more pronounced at higher values of γ. In general, $\overline{Nu}_s$ increases with increase in γ. The difference between Nusselt number of fluid and solid decreases initially with increase in H, and then comes a point when Nusselt number for both fluid and solid are equal, thereafter the difference increases again. It may be noted that the $\overline{Nu}_s$ is a function of conductive as well as radiative heat transfer. The point of zero difference between $\overline{Nu}_f$ and $\overline{Nu}_s$ occurs at lower values of H when γ is increased. Total Nusselt number, $\overline{Nu}_t$ increases with increase in γ.

Fig. 8 shows the average Nusselt number at different values of radiation parameter, R_d. This figure is obtained for $Ra = 100$ and $\gamma = 1$. The Nusselt number of fluid decreases owing to increase in the radiation parameter. The difference between $\overline{Nu}_f$ at various values of R_d is larger at higher value of H. The Nusselt number of solid increases with an increase in radiation parameter. This happens due to the reason that the radiation-conduction effect increases with increased radiation parameter thus increasing the $\overline{Nu}_s$. Owing to increased $\overline{Nu}_s$, the total Nusselt number also increases with increase in radiation parameter. Nusselt number for solid increased by 9.9% when R_d is increased from 0 to 0.1 whereas 69% increase in $\overline{Nu}_s$ is observed when R_d is varied from 0.1 to 1.

Fig. 9 illustrates the variation of average Nusselt number with respect to γ and R_d for $Ra = 100$ and $H = 1$. It can be seen that the Nusselt number for fluid is not affected with respect to change in R_d for chosen range of γ values. $\overline{Nu}_f$ remains almost constant when γ is varied from 0.1 to 100. However, $\overline{Nu}_s$ increases with increase in γ. The decrease in thermal conductivity of solid leads to increase in γ. Smaller the thermal conductivity of solid, lesser is the heat diffusion into the solid phase, which in turn forms a thinner thermal boundary layer near the surface of cavity leading to enhanced Nusselt number of solid. Nusselt number of solid increases gradually for $\gamma \leqslant 20$ and thereafter a sharp increase is observed. This increase becomes even sharper at higher values of radiation parameter. The $\overline{Nu}_s$ is more sensitive to changes in γ than that of H. For instance, the variation of γ from 1 to 100 resulted in 95% increase of $\overline{Nu}_s$ where as 40% increase in $\overline{Nu}_s$ is observed when H is varied from 1 to 100, by keeping other variables constant. Total Nusselt number also increase with increase in radiation parameter. The contribution of $\overline{Nu}_s$ is much higher than that of $\overline{Nu}_f$ in increasing $\overline{Nu}_t$. The effect of radiation parameter on total Nusselt number diminishes at higher values of γ. This can be attributed to the reason that the higher value of γ corresponds to higher fluid thermal conductivity compared to that of solid thermal conductivity. The fluid properties dominate at higher value of γ thus major portion of the heat is transferred by fluid and the total Nusselt number is controlled by fluid heat transfer rate. Fig. 10 depicts the effect of Rayleigh number on Nusselt number. This figure is obtained by taking $H = 1$ and $R_d = 0.5$. As shown in this figure the solid and fluid Nusselt numbers increase with increase in Rayleigh number as expected. It is observed that at low Rayleigh number ($Ra = 10$)

the $\overline{Nu}_t$ decreases with the increase in γ. However at higher Rayleigh number $\overline{Nu}_t$ increases with increase in γ.

5. Conclusion

Heat transfer from a square cavity with hot left wall and cold right wall, is investigated using thermal non-equilibrium model. The governing equations are non-dimensionalised and solved using finite element method. Effect of various parameters on Nusselt number such as the inter-phase heat transfer coefficient, modified conductivity ratio, radiation parameter and Rayleigh number are analysed. It is seen that the local Nusselt number for fluid and solid decrease with increase of cavity height at hot wall and vice-versa at cold wall. At hot wall, Nu_f is higher at the bottom part of cavity as compared to Nu_s and vice-versa at upper part of the cavity. However at cold wall, the heat transfer behavior is opposite to that at hot wall. $\overline{Nu}_f$ decreases with increase in H whereas $\overline{Nu}_s$ increases with increase in H. Higher value of H leads to thermal equilibrium between fluid and solid phases. $\overline{Nu}_t$ increases with increase in γ and R_d. Higher value of γ also brings the fluid and solid into state of thermal equilibrium. It is seen that the heat transfer rate from the cavity to solid phase is more sensitive to γ than H. The Nusselt number for solid increases with increase in radiation parameter whereas the Nusselt number for fluid is not affected at lower values of H, but decreases with increase in radiation parameter at higher values of H. The effect of radiation parameter on total Nusselt number diminishes at higher values of γ. Nusselt number for solid and fluid increases with increase in Rayleigh number. $\overline{Nu}_t$ decreases with increase in γ at low Rayleigh number but increases with increase in γ at higher Rayleigh number.

References

[1] D.A. Nield, A. Bejan, Convection in Porous Media, second ed., Springer, New York, 1999.

[2] K. Vafai, Hand Book of Porous Media, Marcel Dekker, New York, 2000.

[3] K. Vafai, Handbook of Porous Media, second ed., Taylor & Francis Group, Boca Raton, FL, 2005.

[4] I. Pop, D.B. Ingham, Convective Heat Transfer: Mathematical and Computational Modeling of Viscous Fluids and Porous Media, Pergamon, Oxford, 2001.

[5] A.C. Baytas, I. Pop, Free convection in a square porous cavity using a thermal nonequalibruim model, Int. J. Thermal Sci. 41 (2002) 861–870.

[6] N.H. Saeid, Analysis of mixed convection in a vertical porous layer using non-equilibrium model, Int. J. Heat Mass Transfer 47 (2004) 5619–5627.

[7] P.-X. Jiang, Z.-P. Ren, Numerical investigation of forced convection heat transfer in porous media using a thermal non-equilibrium model, Int. J. Heat Fluid Flow 22 (2001) 102–110.

[8] D.A.S. Rees, A.P. Bassom, I. Pop, Forced convection past a heated cylinder in a porous medium using a thermal nonequalibruim model: Boundary layer analysis, European J. Mech. B/Fluids 22 (2003) 473–486.

[9] S.W. Wong, D.A.S. Rees, I. Pop, Forced convection past a heated cylinder in a porous medium using a thermal non-equilibrium model: Finite Peclet number effects, Int. J. Thermal Sci. 43 (2004) 213–220.

[10] A. Marafie, K. Vafai, Analysis of non-Darcian effects on temperature differentials in porous media, Int. J. Heat Mass Transfer 44 (2001) 4401–4411.

[11] B. Cherif, M.S. Sifaoui, Numerical study of heat transfer in an optically thick semi-transparent spherical porous medium, Journal of Quantitative Spectroscopy & Radiative Transfer 91 (2005) 363–372.

[12] B. Cherif, M.S. Sifaoui, Theoretical study of heat transfer by radiation conduction and convection in a semi-transparent porous medium in a cylindrical enclosure, Journal of Quantitative Spectroscopy & Radiative Transfer 83 (2004) 519–527.

[13] T. Sghaier, B. Cherif, M.S. Sifaoui, Theoretical study of combined radiative conductive and convective heat transfer in a semi-transparent porous medium in a spherical enclosure, Journal of Quantitative Spectroscopy & Radiative Transfer 75 (2002) 257–271.

[14] A.C. Baytas, Thermal non-equilibrium natural convection in a square enclosure filled with a heat-generating solid phase, non-Darcy porous medium, Int. J. Energy Res. 27 (2003) 975–988.

[15] M.F. Modest, Radiative Heat Transfer, McGraw-Hill, New York, 1993.

[16] A. Raptis, Radiation and free convection flow through a porous medium, Int. Comm. Heat Mass Transfer 25 (1998) 289–295.

[17] L.J. Segerland, Applied Finite Element Analysis, John Wiley and Sons, New York, 1982.

[18] R.W. Lewis, P. Nithiarasu, K.N. Seetharamu, Fundamentals of the Finite Element Method for Heat and Fluid Flow, John Wiley and Sons, Chichester, 2004.

[19] K.L. Walker, Homsy G.M., Convection in a porous cavity, J. Fluid Mech. 87 (1978) 449–474.

[20] A. Bejan, On the boundary layer regime in a vertical enclosure filled with a porous medium, Lett. Heat Mass Transfer 6 (1979) 93–102.

[21] R.J. Gross, M.R. Bear, C.E. Hickox, The application of flux-corrected transport (FCT) to high Rayleigh number natural convection in a porous medium, in: Proceedings of 8th International Heat Transfer Conference, San Francisco, CA, USA, 1986.

[22] D.M. Manole, J.L. Lage, Numerical benchmark results for natural convection in a porous medium cavity, in: Heat and Mass Transfer in Porous Media, ASME Conference, in: HTD, vol. 216, 1992, pp. 55–60.

[23] C. Bekermann, R. Viskanta, S. Ramadhyani, A numerical study of non-Darcian natural convection in a vertical enclosure filled with a porous medium, Numer. Heat Transfer Part A 10 (1986) 557–570.

[24] S.L. Moya, E. Ramos, M. Sen, Numerical study of natural convection in a tilted rectangular porous material, Int. J. Heat Mass Transfer 30 (1987) 741–756.

[25] A.C. Baytas, I. Pop, Free convection in oblique enclosures filled with a porous medium, Int. J. Heat Mass Transfer 42 (1999) 1047–1057.

[26] A. Misirlioglu, A.C. Baytas, I. Pop, Free convection in a wavy cavity filled with a porous medium, Int. J. Heat Mass Transfer 48 (2005) 1840–1850.